Real-time estimation of the effective reproduction number of SARS-CoV-2 in Aotearoa New Zealand

Rachelle N Binny [Corresp., Equal first author, 1, 2] , **Audrey Lustig** [Equal first author, 1, 2] , **Shaun C Hendy** [1, 3] , **Oliver J Maclaren** [4] , **Kannan M Ridings** [1, 3] , **Giorgia Vattiato** [1, 3, 5] , **Michael J Plank** [1, 5]

[1] Te Pūnaha Matatini, Auckland, New Zealand

[2] Manaaki Whenua-Landcare Research, Lincoln, New Zealand

[3] Department of Physics, University of Auckland, Auckland, New Zealand

[4] Department of Engineering Science, University of Auckland, Auckland, New Zealand

[5] School of Mathematics and Statistics, University of Canterbury, Christchurch, New Zealand

Corresponding Author: Rachelle N Binny
Email address: binnyr@landcareresearch.co.nz

During an epidemic, real-time estimation of the effective reproduction number supports decision makers to introduce timely and effective public health measures. We estimate the time-varying effective reproduction number, R_t, during Aotearoa New Zealand's August 2021 outbreak of the Delta variant of SARS-CoV-2, by fitting the publicly available EpiNow2 model to New Zealand case data. While we do not explicitly model non-pharmaceutical interventions or vaccination coverage, these two factors were the leading drivers of variation in transmission in this period and we describe how changes in these factors coincided with changes in R_t. Alert Level 4, New Zealand's most stringent restriction setting which includes stay-at-home measures, was initially effective at reducing the median R_t to 0.6 (90% CrI 0.4, 0.8) on 29 August 2021. As New Zealand eased certain restrictions and switched from an elimination strategy to a suppression strategy, R_t subsequently increased to a median 1.3 (1.2, 1.4). Increasing vaccination coverage along with regional restrictions were eventually sufficient to reduce R_t below 1. The outbreak peaked at an estimated 198 (172, 229) new infected cases on 10 November, after which cases declined until January 2022. We continue to update R_t estimates in real time as new case data become available to inform New Zealand's ongoing pandemic response.

1 Real-time estimation of the effective reproduction number of SARS-

2 CoV-2 in Aotearoa New Zealand

4 Binny RN[Corresp., Equal first author,1,2], Lustig A[Equal first author,1,2], Hendy SC[2,4], Maclaren OJ[5], Ridings

5 KM[2,4], Vattiato G[2,3,4], Plank MJ[2,3]

7 [1]Manaaki Whenua-Lancare Research, Lincoln, New Zealand.

8 [2]Te Pūnaha Matatini, Centre of Research Excellence in Complex Systems, New Zealand.

9 [3]School of Mathematics and Statistics, University of Canterbury, New Zealand.

10 [4]Department of Physics, University of Auckland, New Zealand.

11 [5]Department of Engineering Science, University of Auckland, New Zealand.

13 Corresponding Author:
14 Rachelle Binny
15 Manaaki Whenua, PO Box 69040, Lincoln 7640, New Zealand.
16 Email address: binnyr@landcareresearch.oc.nz
17

19 **Abstract**

20 During an epidemic, real-time estimation of the effective reproduction number supports decision

21 makers to introduce timely and effective public health measures. We estimate the time-varying

22 effective reproduction number, R_t, during Aotearoa New Zealand's August 2021 outbreak of the

23 Delta variant of SARS-CoV-2, by fitting the publicly available EpiNow2 model to New Zealand

24 case data. While we do not explicitly model non-pharmaceutical interventions or vaccination

25 coverage, these two factors were the leading drivers of variation in transmission in this period

26 and we describe how changes in these factors coincided with changes in R_t. Alert Level 4, New

27   Zealand's most stringent restriction setting which includes stay-at-home measures, was initially

28   effective at reducing the median R_t to 0.6 (90% CrI 0.4, 0.8) on 29 August 2021. As New

29   Zealand eased certain restrictions and switched from an elimination strategy to a suppression

30   strategy, R_t subsequently increased to a median 1.3 (1.2, 1.4). Increasing vaccination coverage

31   along with regional restrictions were eventually sufficient to reduce R_t below 1. The outbreak

32   peaked at an estimated 198 (172, 229) new infected cases on 10 November, after which cases

33   declined until January 2022. We continue to update R_t estimates in real time as new case data

34   become available to inform New Zealand's ongoing pandemic response.

35

36   **Introduction**

37   An important measure in epidemiology is the reproduction number. The basic reproduction

38   number, R_0, is the average number of people infected by a single infected individual, in a fully

39   susceptible population and in the absence of any public health measures. For the highly

40   transmissible Delta variant of SARS-CoV-2 (the virus that causes COVID-19), R_0 is estimated to

41   be at least 6, compared to around 2.5-3 for the original strain of the virus. In reality, the

42   proportion of the population who have immunity to the virus, either through infection or

43   vaccination, changes during the course of an epidemic and transmission can be altered by

44   introduction of public health measures, such as facemask use, contact tracing, quarantining

45   infectious individuals, stay-at-home orders, and school or workplace closures. The effective

46   reproduction number, R_t, is the average number of people infected by a single infected individual

47   at a particular time t, accounting for this partial population immunity and changes in

48   transmission levels due to public health measures.

49   Tracking estimates of the effective reproduction number in real time is useful for: 1) estimating

50   how quickly an outbreak is likely to grow or shrink under current public health measures, to

51   inform decisions on whether measures need to be escalated or scaled back, and 2) assessing the

52   effectiveness of these measures for reducing transmission. Different models have been developed

53   for estimating R_t from time-series data on the number of reported cases. Each model comes with

54   its own set of assumptions and limitations, therefore it is useful for decision makers to have a

55   range of estimates from different models to compare. One such model, implemented in the

56   EpiNow2 package in R statistical software (S. Abbott, J. Hellewell, K. Sherratt, et al., 2020; S.

57   Abbott, J. Hellewell, R. N. Thompson, et al., 2020; R Core Team, 2021), follows current best

58   practices (Gostic et al., 2020) to provide estimates of the time-varying instantaneous

59   reproduction number, case growth rate, doubling time, and case numbers by date of infection.

60   Their modelling approach is based on a method by Cori et al. (2013) and Thompson et al. (2019),

61   extended to account for delays from infection to reporting.

62   From the start of the COVID-19 pandemic until the end of 2021, New Zealand pursued an

63   elimination strategy (Baker et al., 2020). This involved a four-tier alert level system of

64   restrictions (Unite against COVID-19, 2022b), including nationwide and regional lockdown

65   measures, which successfully eliminated community transmission of SARS-CoV-2 during

66   outbreaks in March-May 2020, August-September 2020 and February-March 2021. On 17

67   August 2021, after several months with no known community transmission, New Zealand

68   detected its first case of the Delta variant in the community, in a 58-year old man with no clear

69   link to the border. At that time, only 38% of the population had received at least one vaccine

70   dose, which would have been insufficient to prevent a large outbreak occurring without strong

71   public health measures in place (Steyn, Hendy, et al., 2021; Steyn et al., 2022). The government

72   therefore made the decision to move the entire country into Alert Level 4, the most stringent tier

73   of restrictions (Table 1). Over the following days, contact tracing and surveillance testing efforts

74   were ramped up in an attempt to ring-fence the outbreak as daily case numbers rapidly increased

75   to 79 new cases on 26 August. Whole genome sequencing later identified possible links to

76   infected travellers who arrived at a managed isolation and quarantine (MIQ) facility from New

77   South Wales, Australia (Jelley et al, 2022).

78   Ten days after the introduction of Alert Level 4 restrictions, daily cases levelled off then steadily

79   declined. Results from widespread community testing and wastewater testing suggested the

80   outbreak was so far contained within Auckland and on 1 September regions outside of Auckland

81   began a phased easing to Alert Level 2. Over the following weeks, daily case numbers dwindled

82   in a long outbreak tail, with 10-20 new cases reported each day. However, elimination proved

83   more difficult than previous outbreaks of earlier variants, particularly when transmission started

84   to occur within unvaccinated groups in emergency and transitional housing, where public health

85   measures including contact tracing and self-isolation were more challenging or impossible. From

86   22 September, restrictions in Auckland were eased to Alert Level 3 and, following detections in

87   the neighbouring regions of Waikato and Northland, these regions moved up to Alert Level 3.

88   On 6 October, despite a rise in case numbers, the government announced further easing of some

89   restrictions for Auckland and case numbers continued to steadily grow. This decision marked a

90   transition from New Zealand's elimination strategy to one of suppression: using restrictions to

91   control case numbers to low levels while continuing to increase vaccination coverage in the

92   population through an accelerated vaccine roll-out. Modelling suggested that well over 90% of

93   New Zealand's eligible population, aged 12 years and over, need to be fully vaccinated (two

94   vaccine doses) to safely control community transmission without the need for strong public

95   health measures, such as stay-at-home orders and workplace closures (Steyn, Plank, et al., 2021;

96   Steyn et al., 2022). By mid-November, with close to 80% of the eligible population vaccinated

97   with two doses and all regions except Auckland at Alert Level 2, the Delta outbreak reached its

98   peak at approximately 200-220 new cases per day. Cases steadily declined from this time until

99   January 2022 and by 18 January there were a total of 11,396 reported community cases and 26

100   deaths related to the Delta outbreak. The four-tier Alert Level system was replaced with a 3-tier

101   COVID-19 Protection Framework (Unite against COVID-19, 2022a) (traffic light levels, with

102   red being the highest restriction setting, focused on minimising spread and providing protection

103   through high vaccination coverage) which came into effect on 2 December 2021. Following the

104   detection of nine community cases infected with the highly transmissible Omicron variant

105   announced on 23 January, cases numbers rapidly increased again and New Zealand experienced

106   its largest COVID-19 outbreak to date, peaking in mid-March 2022.

107

108   The ability to track changes in case numbers and the reproduction number in real time is critical

109   to inform decisions about when and where additional measures should be introduced to prevent

110   high case numbers overwhelming healthcare and contact tracing systems, and when these

111   measures can be safely eased. In this work, we use EpiNow2 to estimate the time-varying

112   effective reproduction number R_t in New Zealand during the August 2021 - January 2022

113   outbreak of the Delta variant. The EpiForecasts team who developed EpiNow2, apply the model

114   to global, publicly available case data, aggregated using the covidregionaldata R package (Sam

115   Abbott et al., 2020; R Core Team, 2021), and publish real-time estimates of the effective

116   reproduction number on their webpage (https://epiforecasts.io/covid/) (S. Abbott, J. Hellewell, R.

117   N. Thompson, et al., 2020). However, there is value in applying this method using more detailed

118   line list data held by Ministry of Health, which allows model parameters to be tailored

119   specifically to the New Zealand setting. We compare our estimates to these EpiForecasts

120   estimates and summarise the differences in assumptions made in our implementation of the

121   model. Throughout New Zealand's Delta outbreak and in the current Omicron outbreak, we

122   continue to update our estimates regularly as new data become available and provide these to

123   Ministry of Health to inform operational planning and decision-making in real time.

124   **Materials & Methods**

125   *Data*

126   Data on daily numbers of COVID-19 cases in New Zealand's Delta outbreak, extracted from the

127   EpiSurv database (administered by ESR), were obtained from Ministry of Health (MOH). Data

128   fields included the date of reporting, date of symptom onset (where available), whether the case

129   was internationally-imported (yes, no or unknown), and status ('confirmed', 'probable' or 'under

130   investigation'). Only confirmed and probable cases were included in our analyses. The EpiSurv

131   database is updated in real time and cases 'under investigation' generally arise in the last 1-3

132   days of each instance of the database; in subsequent updates, they are either removed or updated

133   to 'confirmed' or 'probable'. Exclusion of these cases may introduce a downward bias in

134   effective reproduction number estimates at the end of the time-series. However, cases under

135   investigation may include some individuals who ultimately test negative and reporting practices

136   may vary consistently between different District Health Boards so these data cannot be reliably

137   included.

138   Here, we analyse data extracted from the EpiSurv database on 20 January 2022 on all cases

139   (n=12,460; 12,441 confirmed, 19 probable, 0 under investigation) reported between 17 August

140   2021 and 19 January 2022. Case data on the last day of the time-series (n=50) are likely right-

141   truncated due to an unrecorded delay between a case returning a positive test result and being

142   recorded in the dataset. For input to the model, we therefore truncated the time series to exclude

143   the last day of data. We also excluded the internationally-imported cases (n=1014), all of which

144   were detected in MIQ and had no exposure to the community. This left 11,378 confirmed cases

145   and 18 probable cases in the line list which were aggregated to give the daily totals of new

146   reported cases.

147

148   ***Model***

149   We implement the EpiNow2 package S. Abbott, J. Hellewell, K. Sherratt, et al. (2020) to

150   estimate a time-varying effective reproduction number, R_t, during New Zealand's Delta

151   outbreak, using data on daily reported case numbers from 17 August 2021 to 18 January 2022. A

152   detailed description of the model is given in S. Abbott, J. Hellewell, R. N. Thompson, et al.

153   (2020). EpiNow2 implements a Bayesian latent variable approach, with the following key

154   modelling steps:

155   1. Starting with an estimate of the initial number of infections (with a prior based on initial

156   case numbers), incidence is projected forward in time on a daily time step. Here,

157   incidence is defined as the number of individuals who are infected at time t, and who will

158   eventually be tested and reported as a case. We do not model undetected infections, such

159   as asymptomatic infections, that do not appear in case data. The incidence, I_t, at time t is

160   estimated by summing over the imputed incidences $I_{t-\tau}$ from previous time steps τ,

161   weighted by the generation time distribution, and multiplying by the estimate of R_t at

162   time t.

163   2. Temporal variation in R_t is accounted for using an approximate Gaussian process: $R_t \sim R_{t-1} \times$ [squared exponential kernel].

164

165   3. These incidences I_t are mapped to the mean reported cases, D_t, at time t by convolving

166   over the incubation period distribution and the onset-to-reporting delay distribution.

167  4. The observed number of reported cases, C_t, at time t is assumed to be negative-

168   binomially distributed with overdispersion ϕ and mean $(D_t\omega_{d,t})$, where $\omega_{d,t}$ is a day of the

169   week effect (i.e. seven independent parameters) that scales the mean reported cases at

170   time t according to the day of the week.

171

172 Following S. Abbott, J. Hellewell, R. N. Thompson, et al. (2020), we employ a gamma-

173 distributed generation time distribution sourced from Ganyani et al. (2020) but refit using the

174 log-normal incubation period distribution reported by Lauer et al. (2020) with mean 5.2 (SD 1.1)

175 days and SD of 1.52 (SD 1.1) days. This results in a mean generation time of 3.6 (SD 0.7) days

176 and standard deviation 3.1 (SD 0.8) days. Both Ganyani et al. (2020) and Lauer et al. (2020) used

177 data on the original strain of SARS-CoV-2. An analysis of household transmission data by Hart

178 et al. (2022) estimated a mean intrinsic generation time for the Delta variant of 4.7 (95% CrI 4.1,

179 5.6) days and a mean household generation time of 3.2 (2.5, 4.2) days, which were lower than

180 estimates for the Alpha variant (5·5 [4·7, 6·5] days and 4·5 [3·7, 5·4] days for intrinsic and

181 household generation times respectively). We refit the model using these shorter and longer

182 mean generation times to assess to what extent it affected our results.

183 The delay from symptom onset to reporting is estimated by fitting a log-normal distribution,

184 using Stan (Stan Development Team, 2020), to 100 subsampled bootstraps of the onset-to-report

185 delays from 3208 cases reported between 17 August 2021 and 18 January 2022 (excluding 9

186 cases with delays greater than 60 days), taking (with replacement) 250 samples from these delays

187 in each bootstrap. The distribution is adjusted to account for left and right censoring in the data

188 due to dates being rounded to the nearest day. For computational reasons, the distribution is

189 truncated to the maximum observed delay. In preliminary analyses, we checked for temporal

190   variation in reporting delays by performing independent fits of a log-normal distribution to the

191   delays recorded in each month. There was little change in distribution parameters between

192   different months (Table S2) so we assumed the delay distribution was static over the full time

193   period. There was insufficient data to assess whether delays varied spatially. The model was

194   fitted to the time-series of new reported cases per day using Markov-chain Monte Carlo

195   (MCMC), implemented in Stan (Stan Development Team, 2020). We used four chains with a

196   warmup of 500 steps each and 4000 samples post-warmup. Convergence was assessed using the

197   R hat diagnostic.

198   The model outputs the posterior estimates of the inferred incidence I_t (i.e. new cases at their time

199   of infection), the mean reported cases $D_t \omega_{d,t}$, (i.e. new cases at their time of reporting, having

200   accounted for incubation periods, reporting delays, and day of the week effects) and the

201   instantaneous effective reproduction number R_t over the modelled time period. The latter is

202   defined as the expected number of new secondary infections per infectious individual at time t,

203   scaled by their relative infectiousness at time t (Gostic et al., 2020). Estimates over the last nine

204   days of the time-series are based on partial data because the delays from infection to reporting

205   mean there are very likely some cases who were infected on these dates but have yet to appear in

206   reported case data. The time-varying growth rate, r_t, is also estimated from the time-varying

207   effective reproduction number using an approximation derived by Park et al. (2019). Doubling

208   time (or halving time when growth rate is negative) is calculated as $\ln(2)/r_t$. In Results, we

209   provide figures showing the estimated 20%, 50% and 90% credible intervals (CrI) of the

210   posterior distributions for $(D_t \omega_{d,t})$, I_t, R_t and r_t. We do not explicitly model non-pharmaceutical

211   interventions or vaccination so cannot directly quantify their effects on transmission. However,

212   given that levels of immunity from prior infections were very low during the period studied,

213   these two factors were the leading drivers of variation in transmission in this period so we

214   discuss how changes in R_t coincided with changes in interventions and increasing vaccination

215   coverage. The EpiNow2 package allows forecasting of estimates over a 14-day time horizon but

216   we do not implement that functionality here. Model assumptions and how they differ from the

217   implementation by EpiForecasts, used to generate the New Zealand estimates published on their

218   webpage (https://epiforecasts.io/covid/posts/national/new-zealand/), are detailed in Table 2.

219

220   Results

221   Using subsampled bootstraps of the delays from symptom onset to reporting, up to a maximum

222   of 34 days, we fitted a lognormal distribution of onset-to-report delays with a mean of 3.84 days

223   and standard deviation of 3.94 days (parameters: μ=0.988 (SD=0.088) and σ=0.847 (SD=0.063),

224   which was a good visual match to the data (Figure S1). Fitting the EpiNow2 model to the 22-

225   week time-series of daily reported case numbers, we obtained estimates for the time-varying

226   mean reported cases, incidence, effective reproduction number and growth rate of New

227   Zealand's Delta outbreak up to 18 January 2022. The Rhat statistic was less than 1.05 for all

228   parameter estimates indicating model convergence. The estimated daily number of new cases

229   (ribbons) are shown alongside the actual reported case numbers (grey bars) in Figure 1. Mean

230   reported case counts ($D_t\,\omega_{d,t}$) by date of report (Fig. 1A), were a good visual match to the data,

231   first peaking at a median 57 (90% CrI 32, 90) cases on 27 August 2021 (cf. 79 on 26 August in

232   actual reported cases). Plotting cases by their estimated date of infection (I_t) shows the first peak

233   in incidence occurred on 20 August with a median 73 (48, 101) new cases infected that day (Fig.

234   1B).

235   Figure 2 shows the change in estimated effective reproduction number (R_t) over time alongside

236   key timings of changes to levels of restrictions. On 17 August, R_t is greater than one but

237   immediately starts to decline after introduction of Alert Level 4 restrictions from 18 August.

238   This, along with the decline in incidence from 20 August, suggests that these restrictions had a

239   near-immediate effect on reducing transmission, though this reduction did not filter through to

240   reported case numbers for another 7-10 days. After twelve days under Alert Level 4 restrictions,

241   the median R_t was reduced to 0.57 (0.42, 0.76), growth rate r_t was -0.13 (-0.18, -0.07) per day

242   and doubling time was -5.48 (-3.89, -10.26) days (Fig. 2-3). Estimated daily cases by infection

243   date were reduced to a minimum of 14 (11, 18) per day by 6 September (Fig. 1B) and the

244   outbreak entered its long tail. After this time, the reproduction number and daily infections

245   steadily increased, with R_t growing to values greater than one from 11 September. Coinciding

246   with the further easing of some restrictions in Auckland during September and October, median

247   R_t remained over 1 and New Zealand experienced its largest outbreak since the start of the

248   pandemic. Transmission was at its highest on 2 October, with median R_t = 1.27 (1.15, 1.38),

249   corresponding to a growth rate of 0.07 (0.04, 0.10) per day and doubling time of 9.66 (16.68,

250   6.86) days. However, by mid-November, regional Alert Level 3 restrictions remained in place

251   and vaccination coverage had rapidly increased from 38% of the eligible population having

252   received at least one vaccine dose on 17 August to 89% by 10 November. The median R_t

253   subsequently decreased below 1, causing the outbreak to peak at an estimated 198 (172, 229)

254   new cases infected on 10 November (cf. 226 cases reported on 10 November in actual data).

255   From this point, median R_t remained relatively constant at around 0.8 to 0.9 as cases continued to

256   decline and the COVID-19 Protection Framework was introduced. By January 2022, prior to

257   detection of community cases with the Omicron variant, the outbreak had decreased to a median

258   20-30 cases infected per day.

259   Note that during the first 6.5 weeks of the outbreak, the vast majority of reported cases were

260   detected only in the Auckland region. On 3 October, cases were detected in Waikato and from

261   this time on transmission occurred within both regions but likely not between the two regions

262   due to the Auckland travel boundary in place until 14 December. This is supported by whole

263   genome sequencing which suggested that the Waikato cluster arose from a single introduction

264   from Auckland (Hadfield et al., 2018; Khare et al., 2021), while clusters detected in Northland in

265   late October – early November likely represented multiple introductions (Ministry of Health,

266   2021).

267   Refitting the model using the mean generation times of Hart et al. (2022) resulted in similar

268   estimates of R_t as shown in Figure S3. With the shorter mean generation time of 3.2 days, R_t

269   reached its minimum at a median 0.73 (0.53, 0.83) on 30 August and its maximum of 1.24 (1.15,

270   1.32) on 1 October. Assuming a longer mean generation time of 4.6 days resulted in a minimum

271   R_t of 0.52 (0.40, 0.72) on 30 August and maximum on 1.32 (1.18, 1.46) on 5 October. Summary

272   statistics for all posterior estimates are provided in Table S1.

273   Estimates of daily numbers of reported cases by report date and infection date, and the effective

274   reproduction number published by EpiForecasts are shown in Figure S2, for two 16-week

275   periods up to 15 October 2021 and up to 28 January 2022. The EpiForecasts estimates were

276   broadly similar to our estimates but tended to over-estimate the numbers of new infections each

277   day, particularly in periods of low local transmission. Epiforecasts fit to data published by the

278   World Health Organisation (World Health Organisation, 2020), which sources data from the

279   New Zealand Ministry of Health (Ministry of Health, 2022), but does not include information on

280   the importation status of New Zealand's cases. Case numbers modelled by EpiForecasts were

281   therefore biased upwards by inclusion of internationally-imported cases detected in MIQ

282 facilities. As the EpiForecasts model attributes all new imported cases to local transmission, this

283 could result in over- or under-estimation of R_t. We were able to isolate the domestically-acquired

284 cases for model fitting to provide less biased estimates of community transmission occurring in

285 New Zealand.

286

287

288 **Discussion**

289 Our study demonstrates how real-time estimation of the effective reproduction number can

290 effectively support a timely public health response during a community outbreak. New Zealand's

291 elimination strategy and use of stringent stay-at-home measures were successful at controlling

292 several outbreaks of earlier variants even while vaccination coverage remained low. However,

293 they were less effective at controlling the highly transmissible Delta variant and an accelerated

294 vaccination rollout in combination with ongoing regional restrictions were ultimately required to

295 reduce R_t below one. For community outbreaks where a significant proportion of cases are

296 internationally-imported, models should distinguish between imported and domestic infections to

297 avoid biasing estimates of transmission.

298

299 Delays from infection to reporting mean that cases reported on a particular day are really

300 indicative of the transmissibility approximately 7-10 days prior. The EpiNow2 framework

301 accounts for these delays, allowing case counts to be mapped from their date of reporting to date

302 of infection to estimate an instantaneous measure of transmissibility under current conditions.

303 While there can be larger uncertainty around R_t estimates closer to 'now' (due to these estimates

304 being based on less data), the EpiNow2 approach is particularly well-suited for informing real-

305 time decisions and facilitating a rapid public health response to changes in transmission. It also

306   allows observed changes in R_t to be related to changes in interventions or other variables

307   affecting transmission at certain times. More naive approaches that estimate the reproduction

308   number directly from reported cases without accounting (or only partially accounting) for these

309   delays provide a lagged view of an outbreak's trajectory and may obscure the temporal

310   relationship between changes in policy or behaviour and transmission dynamics (Gostic et al,

311   2020).

312

313   The instantaneous reproduction number R_t estimated by EpiNow2 is a property of the epidemic

314   at a particular time t. It measures the average number of secondary infections per infectious

315   individual at time t, assuming that the current conditions remain unchanged until those

316   individuals who were infectious at time t have recovered. This differs from another widely

317   computed measure, the case reproduction number R_c, which is the average number of people an

318   individual infected at time t eventually infects, with no assumption of conditions being

319   unchanged after time t. R_c is the measure estimated by Wallinga and Teunis-type methods,

320   though Wallinga and Teunis (2004) consider individuals with symptom onset at time t as

321   opposed to infection at t (Cori et al., 2013). In a situation where a change in conditions (such as

322   the introduction of stay-at-home measures) brings about an abrupt change in transmissibility, the

323   instantaneous reproduction number R_t will also change abruptly at that time. In contrast, R_c will

324   transition smoothly because it estimates the number of people each case will actually infect,

325   accounting for the fact that the infectious periods of cases infected prior to the change in

326   conditions may span times before and after this change in transmission. Estimates of R_c rely on

327   information about future incidence so can only be obtained in retrospect, and suffer from right

328   censoring of reported case data in an epidemic that is still in progress. For estimates of the

329   instantaneous R_t, which are calculated from current and past incidence, right censoring causes

330   fewer issues, especially where the delays to reporting are accounted for; this measure is therefore

331   more appropriate for tracking transmissibility in real-time (Fraser, 2007).

332

333   There are several important limitations of the EpiNow approach. First, the model assumes that

334   the proportion of infections that are detected remains constant over the study period, i.e.

335   consistent methods and effort for surveillance (e.g. testing, contact tracing) and following

336   consistent case definitions. This is assumption is likely violated; in reality, the level of under-

337   reporting varies over time as contact tracing efforts are ramped up and surveillance testing rates

338   vary over time and over different regions. This was certainly the case over the first few weeks of

339   the outbreak. However, such changes will only bias estimates temporarily if surveillance

340   becomes consistent again after a change. The period of time required before estimates become

341   unbiased depends on the generation time distribution, the delay distributions, and the correlation

342   length scale of the Gaussian process used to model temporal variation in R_t.

343   Model estimates are sensitive to the choice of distribution for the delay from symptom onset to

344   reporting. This distribution affects the upscaling of cases by date of onset that accounts for cases

345   that have onset but have yet to be reported. We used a distribution estimated by fitting to data

346   from New Zealand's Delta outbreak. Reporting delays can vary over the course of an outbreak or

347   between regions, especially early on in an outbreak or during periods of high transmission where

348   the testing and contact tracing system may come under significant strain. The model assumes this

349   distribution is static over time, which was a reasonable assumption for this outbreak (Table S2)

350   but may not hold for future outbreaks in New Zealand or in other countries. If the true delay

351   from onset to reporting at a given time is shorter than the estimated static delay distribution, then

352 the model will overestimate onset case numbers, and vice versa for true delays longer than the

353 distribution used. The bootstrapped subsampling approach somewhat mitigates these issues by

354 allowing multiple delay distributions based on the observed data to be considered at the cost of

355 increasing uncertainty in the estimates. However, if significant temporal or spatial variation in

356 reporting delays is suspected in future outbreaks then using other estimation procedures that are

357 robust to such changes (see e.g. Li and White, 2021; Günther et al, 2021) may be more

358 appropriate.

359

360 Using distributions of the incubation period and onset-to-reporting delay to infer incidence from

361 observed reported cases tends to result in over-smoothing of the incidence. The assumed

362 distributions for generation time and incubation period sourced from Ganyani et al. (2020) and

363 Lauer et al. (2020) were estimated by fitting to data on infections with the original strain of the

364 virus in other countries and these distributions may differ for the Delta variant. However, the

365 mean generation time used here sits between two estimates for Delta reported by Hart et al.

366 (2022) and re-ftting the model using these alternative mean generation times had little impact on

367 our estimates of R_t. Furthermore, the model incorporates uncertainty in the means and standard

368 deviations of both distributions (as well as in the reporting delay distribution), which goes some

369 way to accounting for variation from the expected distributions, for example due to different

370 populations or variants. For analyses of future outbreaks, parameters for the incubation period,

371 generation time and reporting delay distributions should continue to be calibrated using up-to-

372 date data as it becomes available. In particular, recent studies have suggested the mean

373 generation time for the Omicron variant may be shorter than the Delta variant (Abbott et al.,

374 2022).

375

376   As with most models, EpiNow2 estimates are more reliable when daily case numbers are large

377   and the time series contains at least 14 days of non-zero cases. When analysing small outbreaks,

378   slight changes in daily case numbers can lead to large variations in model estimates. Such

379   estimates should be treated with caution and interpreted alongside other information sources, for

380   example the detailed case-specific information collected by contact tracers. Case numbers were

381   too low to robustly estimate regional trends during New Zealand's Delta outbreak using this

382   technique. We were able to obtain reliable estimates at national scale, though the estimates based

383   on partial data (orange bands in Figures) in the last 9 days of the time-series are relatively

384   unstable and sensitive to the number of reported cases on the final time point. These values may

385   change significantly as data are updated and new time points are added to the series.

386

387   We do not explicitly model interventions or vaccination so could not establish their relative

388   contributions for reducing transmission. Other models attempting to infer the relative

389   effectiveness of interventions and vaccination (see e.g. Li et al, 2022) generally require data from

390   multiple countries that have implemented similar measures and with varying levels of

391   vaccination coverage. As well as changes to levels of restrictions and vaccination, other factors

392   can also make it challenging to attribute a change in R_t to a particular public health measure. For

393   example, variability in the level of compliance with public health measures over time (eg.

394   willingness to wear facemasks, adherence to restrictions on between-household contact) and

395   between different subgroups in the population influences R_t. Transmission levels will also vary

396   between subgroups of the population, due to different demographics, levels of vaccination, and

397   different environmental conditions, such as average household size and density of housing. The

398 model masks this heterogeneity so the estimates of the time-varying R_t are an attribute of the

399 outbreak, in whichever subgroups it is occurring at that particular time. This has important

400 implications for small outbreaks, where the subgroups in which the virus is spreading may not be

401 representative of the wider population. If case numbers are high enough for reliable inference,

402 such fragmented outbreaks may be better modelled as separate local outbreaks, for example

403 regional-level models for different district health boards (Vegvari et al., 2021). In New Zealand's

404 Delta outbreak, different sub-clusters have been identified (Jelley et al, 2022) but there were

405 insufficient case numbers to fit the model for each sub-cluster separately. It is therefore not

406 possible to disentangle the relative contributions that public health measures and compliance

407 levels had on transmission, from other attributes of the sub-clusters dominating the outbreak at

408 that particular point in time. For example, the increase in transmission towards the end of

409 September could have been driven by the easing of restrictions in Auckland, changing levels of

410 public compliance, the virus spreading into under-vaccinated groups or populations staying in

411 emergency and transitional housing, or the combination of these factors.

412

Conclusions

413
414 Our analysis of New Zealand case data demonstrates the effectiveness of high vaccination

415 coverage in combination with public health measures for controlling an outbreak of the Delta

416 variant of SARS-CoV-2. Modelling approaches that account for delays from infection to

417 reporting reveal important changes in underlying transmission dynamics that may not be

418 apparent when dealing only with reported cases. Real-time estimation of the effective

419 reproduction number remains critical for informing decision-making and operational planning in

420 New Zealand's ongoing pandemic response.

421

Data Availability

The daily case numbers used in this analysis were obtained from an instance of the EpiSurv

database on 20 January 2022, and are provided in the Supplementary Material. The New Zealand

Ministry of Health also publish publicly available case data at

https://github.com/minhealthnz/nz-covid-data/blob/main/cases/covid-cases.csv

Acknowledgements

The authors acknowledge the support of the New Zealand Ministry of Health and the Institute of

Environmental Science and Research in supplying data for these analyses. Results were

generated using the open-source EpiNow2 model developed by S. Abbott, J. Hellewell, K.

Sherratt, et al. (2020), and made use of the estimates and approach of S. Abbott, J. Hellewell, R.

N. Thompson, et al. (2020). We acknowledge the use of New Zealand eScience Infrastructure

(NeSI) high performance computing facilities and consulting support as part of this research.

References

Abbott, S., Hellewell, J., Sherratt, K., Gostic, K., Hickson, J., Badr, H. S., DeWitt, M., Thompson,

R., EpiForecasts, & Funk, S. (2020). EpiNow2: Estimate Real-Time Case Counts and

Time-Varying Epidemiological Parameters. https://doi.org/10.5281/zenodo.3957489

Abbott, S., Hellewell, J., Thompson, R. N., Sherratt, K., Gibbs, H. P., Bosse, N. I., Munday, J. D.,

Meakin, S., Doughty, E. L., Chun, J. Y., Chan, Y.-W. D., Finger, F., Campbell, P., Endo,

A., Pearson, C. A. B., Gimma, A., Russell, T., CMMID COVID modelling group, Flasche,

S., . . . Funk, S. (2020). Estimating the time-varying reproduction number of SARS-CoV-

2 using national and subnational case counts [version 2; peer review: 1 approved with

reservations]. *Wellcome Open Research 5*, 112.

https://doi.org/10.12688/wellcomeopenres.16006.2

447   Abbott, S., Sherratt, K., Bevan, J., Gibbs, H., Hellewell, J., Munday, J., Campbell, P., & Funk, S.

448   (2020). covidregionaldata: subnational data for the COVID-19 outbreak. *10*.

449   https://doi.org/10.5281/zenodo.3957539

450   Abbott, S., Sherratt, K., Gerstung, M., & Funk, S. (2022). Estimation of the test to test distribution

451   as a proxy for generation interval distribution for the Omicron variant in England. *medRxiv*.

452   https://doi.org/10.1101/2022.01.08.22268920

453   Baker, M. G., Kvalsvig, A., Verrall, A. J., & Wellington, N. (2020). New Zealand's COVID-19

454   elimination strategy. *The Medical Journal of Australia*, *213*(5), 198-200.

455   https://doi.org/10.5694/mja2.50735

456   Cori, A., Ferguson, N. M., Fraser, C., & Cauchemez, S. (2013). A new framework and software to

457   estimate time-varying reproduction numbers during epidemics. *American journal of*

458   *epidemiology*, *178*(9), 1505-1512.

459   Fraser, C. (2007). Estimating individual and household reproduction numbers in an emerging

460   epidemic. *PloS one*, *2*(8), e758.

461   Ganyani, T., Kremer, C., Chen, D., Torneri, A., Faes, C., Wallinga, J., & Hens, N. (2020).

462   Estimating the generation interval for coronavirus disease (COVID-19) based on symptom

463   onset data, March 2020. *Eurosurveillance*, *25*(17), 2000257.

464   Gostic, K. M., McGough, L., Baskerville, E. B., Abbott, S., Joshi, K., Tedijanto, C., Kahn, R.,

465   Niehus, R., Hay, J. A., & De Salazar, P. M. (2020). Practical considerations for measuring

466   the effective reproductive number, R_t. *PLoS computational biology*, *16*(12), e1008409.

467   https://doi.org/10.1371/journal.pcbi.1008409

468   Günther, F., Bender, A., Katz, K., Küchenhoff, H., Höhle, M. (2021). Nowcasting the COVID-19

469   pandemic   in   Bavaria. *Biometrical*   *Journal*, 63, 490–

470   502. https://doi.org/10.1002/bimj.202000112

471   Hadfield, J., Megill, C., Bell, S. M., Huddleston, J., Potter, B., Callender, C., Sagulenko, P.,

472   Bedford, T., & Neher, R. A. (2018). Nextstrain: real-time tracking of pathogen evolution.

473   *Bioinformatics*, *34*(23), 4121-4123. https://doi.org/10.1093/bioinformatics/bty407

474   Hart, W. S., Miller, E., Andrews, N. J., Waight, P., Maini, P. K., Funk, S., & Thompson, R. N.

475   (2022). Generation time of the alpha and delta SARS-CoV-2 variants: an epidemiological

476   analysis. *The Lancet Infectious Diseases*. https://doi.org/https://doi.org/10.1016/S1473-

477   3099(22)00001-9

478   Jelley, L., Douglas, J., Ren, X., Winter, D., McNeill, A., Huang, S., French, N., Welch, D.,

479   Hadfield, J., de Ligt, J., & Geoghegan, J. L. (2022). Genomic epidemiology of Delta SARS-

480   CoV-2 during transition from elimination to suppression in Aotearoa New Zealand. *Nature*

481   *Communications*, 13, 4035. https://doi.org/10.1038/s41467-022-31784-5

482   Khare, S., Gurry, C., Freitas, L., Schultz, M. B., Bach, G., Diallo, A., Akite, N., Ho, J., Lee, R. T.,

483   Yeo, W., Curation Team, G. C., & Maurer-Stroh, S. (2021). GISAID's Role in Pandemic

484   Response. *China CDC weekly*, *3*(49), 1049-1051. https://doi.org/10.46234/ccdcw2021.255

485   Kraemer, M., Pigott, D., Xi, B., Hill, S., Gutierrez, B., & Pybus, O. (2020). *Epidemiological data*

486   *from the nCoV-2019 outbreak: Early descriptions from publicly available data*. Retrieved

487   24 March 2022 from https://virological.org/t/epidemiological-data-from-the-ncov-2019-

488   outbreak-early-descriptions-from-publicly-available-data/337

489   Lauer, S. A., Grantz, K. H., Bi, Q., Jones, F. K., Zheng, Q., Meredith, H. R., Azman, A. S., Reich,

490   N. G., & Lessler, J. (2020). The Incubation Period of Coronavirus Disease 2019 (COVID-

491   19) From Publicly Reported Confirmed Cases: Estimation and Application. *Annals of*

492   *Internal Medicine*, *172*(9), 577-582. https://doi.org/10.7326/M20-0504

493 Li, H., Wang, L., Zhang, M., Lu, Y., Wang, W. (2022). Effects of vaccination and non-

494   pharmaceutical interventions and their lag times on the COVID-19 pandemic: Comparison

495   of eight countries. *PLOS Neglected Tropical Diseases,* 16(1),

496   e0010101. https://doi.org/10.1371/journal.pntd.0010101

497 Li T., White L. F. (2021). Bayesian back-calculation and nowcasting for line list data during the

498   COVID-19 pandemic. *PLOS Computational Biology,* 17(7), e1009210.

499   https://doi.org/10.1371/journal.pcbi.1009210

500 Ministry of Health. (2021). *Public health advice on Alert Level settings for Northland and*

501   *Auckland – 7 November*. Retrieved 26 February 2022 from

502   https://covid19.govt.nz/assets/Proactive-Releases/Health-response/10-December-2021/4.-

503   Public-Health-Advice-on-Alert-Level-Settings-for-Northland-and-Auckland-7-

504   November.pdf

505 Ministry of Health. (2022). *COVID-19: curent cases*. Ministry of Health. Retrieved 23 March 2022

506   from https://www.health.govt.nz/our-work/diseases-and-conditions/covid-19-novel-

507   coronavirus/covid-19-data-and-statistics/covid-19-current-cases

508 Park, S. W., Champredon, D., Weitz, J. S., & Dushoff, J. (2019). A practical generation-interval-

509   based approach to inferring the strength of epidemics from their speed. *Epidemics*, *27*, 12-

510   18. https://doi.org/https://doi.org/10.1016/j.epidem.2018.12.002

511 R Core Team. (2021). *R: A language and environment for statistical computing. R Foundation for*

512   *Statistical Computing*. In https://www.R-project.org/Stan Development Team. (2020).

513   *RStan: The r Interface to Stan*. In http://mc-stan.org/

514 Steyn, N., Hendy, S., Plank, M., & Binny, R. (2021). *Technical report: modelling the potential*

515 *spread of COVID-19 during the August 2021 outbreak*. https://cpb-ap-

516 se2.wpmucdn.com/blogs.auckland.ac.nz/dist/d/75/files/2017/01/technical-report-28-

517 august.pdf?_sm_au_=iVVj0Qq3W10PNWvrR6J7NKHB824Vc

518 Steyn, N., Plank, M., & Hendy, S. (2021). *Modelling to support a future COVID-19 strategy for*

519 *Aotearoa New Zealand*. https://cpb-ap-

520 se2.wpmucdn.com/blogs.auckland.ac.nz/dist/d/75/files/2017/01/modelling-to-support-a-

521 future-covid-19-strategy-for-aotearoa-new-

522 zealand.pdf?_sm_au_=iVVnQqtjts1V7nFRR6J7NKHB824Vc

523 Steyn, N., Plank, M. J., Binny, R. N., Hendy, S. C., Lustig, A., & Ridings, K. (2022). A COVID-

524 19 vaccination model for Aotearoa New Zealand. *Scientific Reports*, *12*(1), 2720.

525 https://doi.org/10.1038/s41598-022-06707-5

526 Thompson, R. N., Stockwin, J. E., van Gaalen, R. D., Polonsky, J. A., Kamvar, Z. N., Demarsh,

527 P. A., Dahlqwist, E., Li, S., Miguel, E., Jombart, T., Lessler, J., Cauchemez, S., & Cori, A.

528 (2019). Improved inference of time-varying reproduction numbers during infectious

529 disease outbreaks. *Epidemics*, *29*, 100356.

530 https://doi.org/https://doi.org/10.1016/j.epidem.2019.100356

531 Unite against COVID-19. (2022a). *COVID-19 Protection Framework (traffic lights)*. New

532 Zealand Government. Retrieved 23 February 2022 from https://covid19.govt.nz/traffic-

533 lights/covid-19-protection-framework/

534 Unite against COVID-19. (2022b). *History of the COVID-19 Alert System*. New Zealand

535 Government. Retrieved 23 March 2022 from https://covid19.govt.nz/about-our-covid-19-

536 response/history-of-the-covid-19-alert-system/

537   Vegvari, C., Abbott, S., Ball, F., Brooks-Pollock, E., Challen, R., Collyer, B. S., Dangerfield, C.,

538   Gog, J. R., Gostic, K. M., Heffernan, J. M., Hollingsworth, T. D., Isham, V., Kenah, E.,

539   Mollison, D., Panovska-Griffiths, J., Pellis, L., Roberts, M. G., Scalia Tomba, G.,

540   Thompson, R. N., & Trapman, P. (2021). Commentary on the use of the reproduction

541   number R during the COVID-19 pandemic. *Statistical Methods in Medical Research*,

542   09622802211037079. https://doi.org/10.1177/09622802211037079

543   Wallinga, J., & Teunis, P. (2004). Different Epidemic Curves for Severe Acute Respiratory

544   Syndrome Reveal Similar Impacts of Control Measures. *American journal of*

545   *epidemiology*, *160*(6), 509-516. https://doi.org/10.1093/aje/kwh255

546   World Health Organisation. (2020). *WHO Coronavirus (COVID-19) Dashboard*. World Health

547   Organisation. Retrieved 1 February 2022 from https://covid19.who.int/

548

549

Dates of restrictions and key events following the August 2021 incursion of the Delta variant of SARS-CoV-2 in New Zealand.

Restriction changes occurred at 11.59pm on each date.

1 *Table 1: Dates of restrictions and key events following the August 2021 incursion of the Delta*
2 *variant of SARS-CoV-2 in New Zealand.* *Restriction changes occurred at 11.59pm on each date.*

Date	Restrictions and public health response
17 August 2021	First case of Delta variant detected in the community. Entire country moves to Alert Level 4. Contact tracing, wastewater testing and community testing ramped up. 38% of eligible population (over-12s) has had at least one vaccine dose.
31 August	Regions south of Auckland to Alert Level 3.
2 September	Northland to Alert Level 3.
7 September	Regions outside of Auckland to Alert Level 2.
21 September	Auckland and Upper Hauraki to Alert Level 3.
25 September	Upper Hauraki to Alert Level 2.
3 October	Two cases detected in Raglan and Hamilton. Parts of Waikato move to Alert Level 3.
5 October	Roadmap step 1 introduced in Auckland, allowing up to 10 people from two households to gather outdoors and reopening of Early Childhood Education centres. Transition from elimination strategy to suppression strategy.
7 October	Waikato Alert Level 3 boundary extended to include additional districts.
8 October	Two positive cases are discovered to have travelled out of Auckland into Northland. Northland moves to Alert Level 3.
16 October	'Super Saturday' vaccination drive: 85% of eligible population (aged 12 and over) have had at least one vaccine dose, 66% have received two doses.
19 October	Northland to Alert Level 2.
27 October	Waikato to Step 1 of Alert Level 3. 87% of eligible population have had at least one vaccine dose, 72% have received two doses.
2 November	Upper Northland to Alert Level 3 after detection of two community cases with no known epidemiological links. Waikato to Step 2 of Alert Level 2, allowing up to 25 people from multiple households to meet outdoors. Retail stores and public venues including libraries, museums and zoos can open. Hospitality venues and close contact businesses remain closed.
9 November	Auckland to Step 2 of Alert Level 3.
10 November	89% of eligible population have had at least one vaccine dose, 79% have received two doses.
11 November	Upper Northland to Alert Level 2.
16 November	Waikato to Alert Level 2.
2 December	Introduction of 3-tier COVID-19 Protection Framework (traffic lights). Following regions at Red: Northland, Auckland, Taupō and Rotorua Lakes Districts, Kawerau, Whakatane, Ōpōtiki Districts, Gisborne District, Wairoa District, Rangitikei, Whanganui and Ruapehu Districts. All other regions at Orange. 93% of eligible population have had at least one vaccine dose, 86% have received two doses.
14 December	Auckland travel boundary lifted.

15 December	94% of eligible population have had at least one vaccine dose, 90% have received two doses.
29 December	First border-related Omicron case with community exposures.
30 December	All regions to Orange except Northland.
20 January 2022	Northland to Orange.
23 January	Government announces detection of nine community cases with the Omicron variant and multiple community exposure events.

Model assumptions (those that differ from EpiForecasts in bold text).

1 *Table 2: Model assumptions (those that differ from EpiForecasts in bold text).*

Parameter/dataset	Our implementation	EpiForecasts
Data source	**Ministry of Health line list data from EpiSurv database, administered by ESR. Confirmed and probable cases, excluding internationally-imported cases in MIQ and cases under investigation.**	World Health Organisation (2020) data on confirmed cases, including internationally-imported cases in MIQ.
Model fitting	Four chains with a warmup of 500 each and 4000 samples post-warmup.	
Symptom onset-to-reporting delay distriution	Log-normal distribution with **mean of 3.84 days and standard deviation of 3.94 days [parameters: µ=0.988 (SD=0.088) and σ=0.847 (SD=0.063)]. Maximum delay is 34 days**. Fitted to delays in case data from 17 August 2021 to 18 January 2022; Figure S1.	Log-normal distribution with mean of 6.5 days and standard deviation of 17 days. Maximum delay is 30 days. Fitted to combined data from every country for which onset-to-report delays are available in a publicly accessible linelist (Sam Abbott et al., 2020; Kraemer et al., 2020).
Incubation period distribution	Log-normal with mean of 5.2 days (SD 1.1) and SD of 1.52 days (SD 1.1) (Lauer et al., 2020)	
Generation time distribution	*Main analysis:* Gamma distribution with a mean of 3.64 days (SD 0.71) and SD of 3.07 days (SD 0.77), sourced from Ganyani et al. (2020) but re-fit using Lauer et al. (2020) incubation period. *Shorter generation time:* mean 3.2 (SD 0.46) days and SD 2.4 (0.33) days (Hart et al., 2022). *Longer generation time:* mean 4.6 (SD 0.4) days and SD 3.1 (SD 0.2) days (Hart et al., 2022).	
Prior on R_t at t=0	Log-normal with mean and standard deviation of 1.	
Gaussian process kernel	Squared exponential kernel. Length scale was given a log-normal prior with a mean of 21 days and standard deviation of 7 days truncated to be greater than 3 days and less than the length of the data. The prior on the magnitude was standard normal.	

Figure 1

COVID-19 cases (observed and estimated) over time.

A) Observed cases (confirmed and probable) by date of report (grey bars) and estimated mean reported cases, $D_t\, \omega_{d,t}$, by date of report (ribbon); B) Observed cases by date of report (grey bars) and estimated incidence I_t (cases by date of infection, having accounted for delays from infection to reporting) (ribbon). Lightest ribbon = 90% credible interval (CrI); darker ribbon = 50% CrI; darkest ribbon = 20% CrI. Estimates up to 9 January 2022 are based on full data (green); estimates from 10 January to 18 January (orange) are based on partial data and have been adjusted for right truncation of infections.
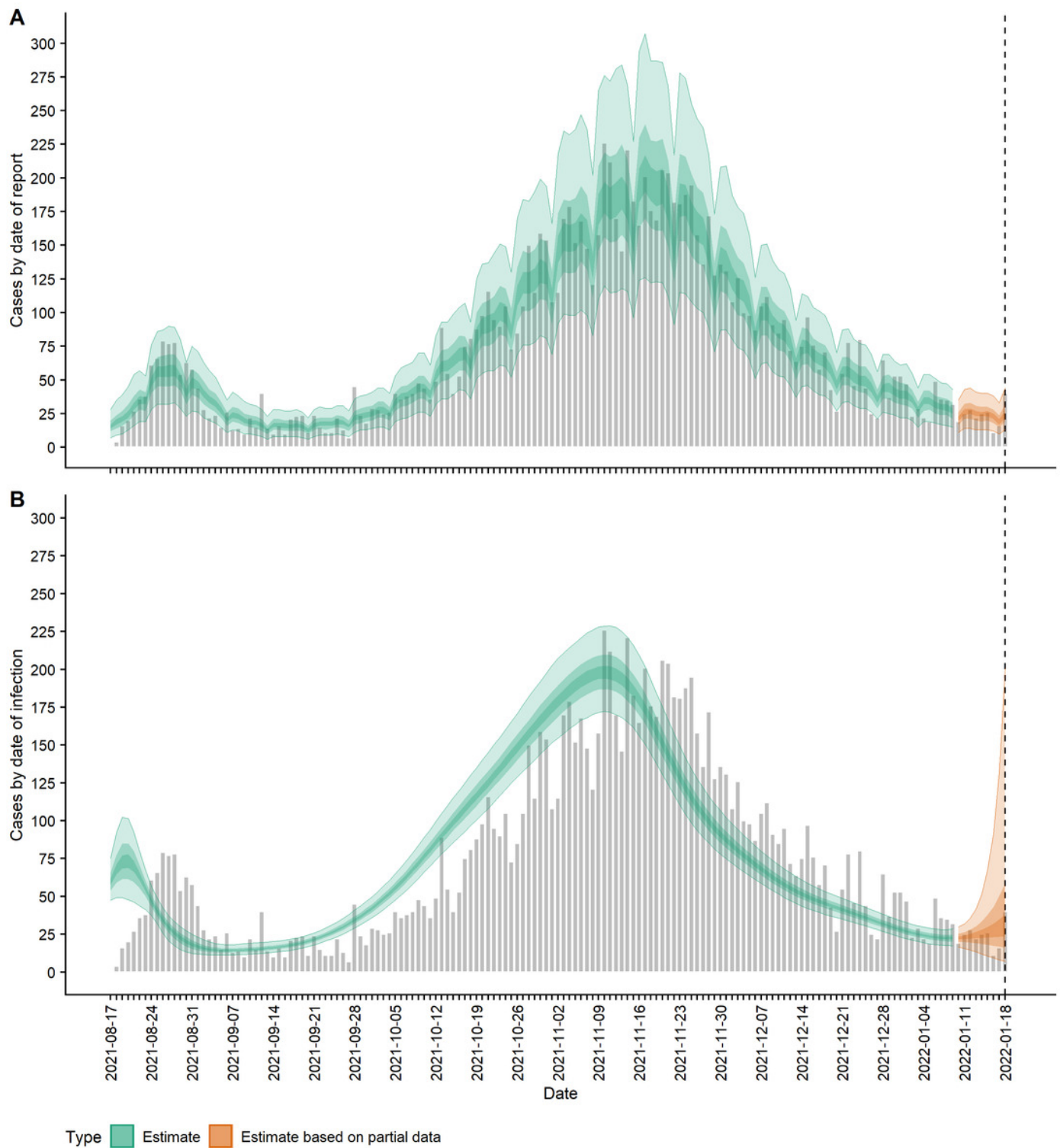
Figure 2

Estimated effective reproduction number, R_t, over time and timings of interventions.

Lightest ribbon = 90% credible interval (CrI); darker ribbon = 50% CrI; darkest ribbon = 20% CrI. Estimates up to 9 January 2022 are based on full data (green); estimates from 10 January to 18 January (orange) are based on partial data and have been adjusted for right truncation of infections.
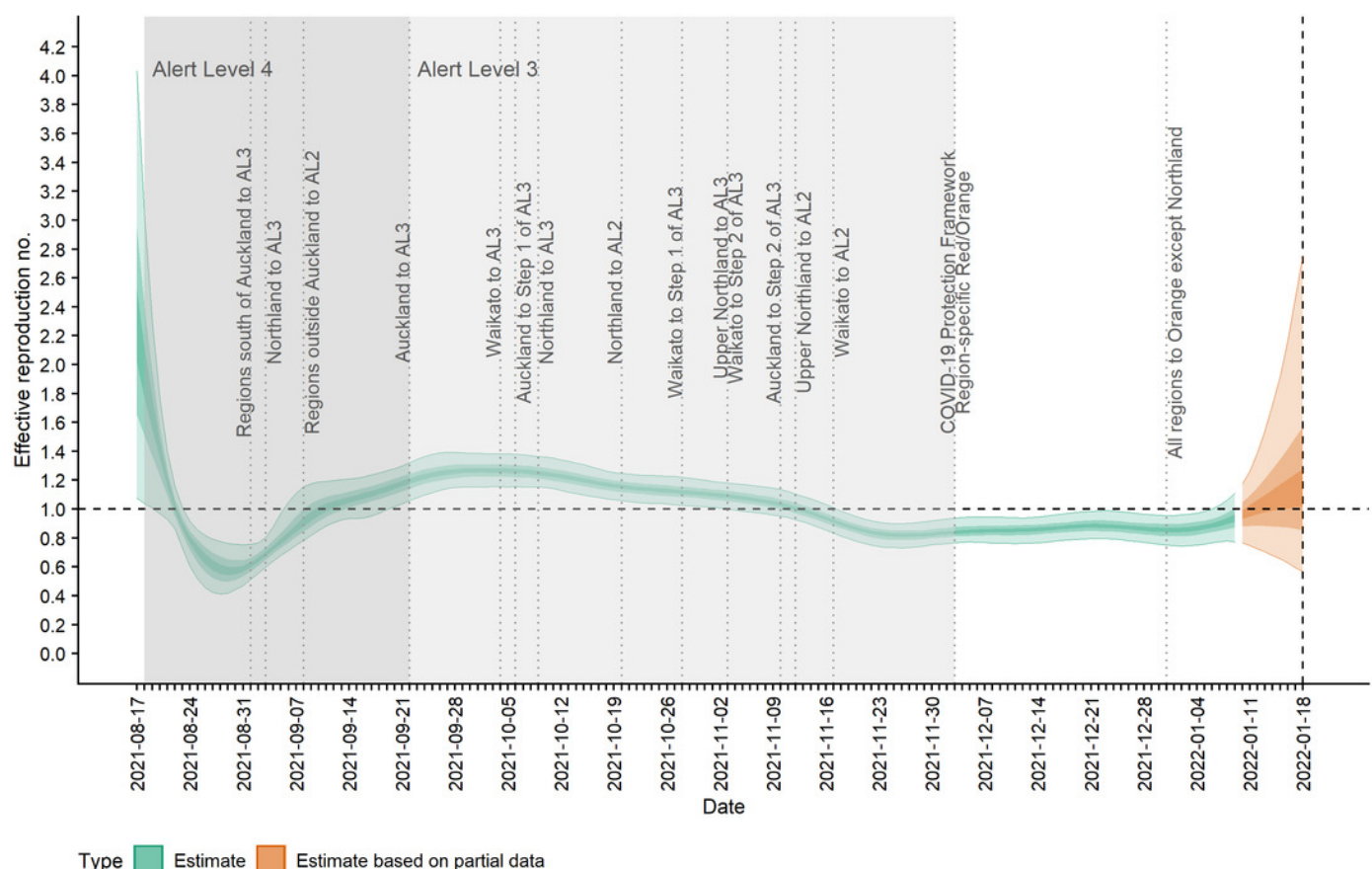
Figure 3

Estimated rate of exponential growth, r_t, over time and timings of interventions.

Lightest ribbon = 90% credible interval (CrI); darker ribbon = 50% CrI; darkest ribbon = 20% CrI. Estimates up to 9 January 2022 are based on full data (green); estimates from 10 January to 18 January (orange) are based on partial data and have been adjusted for right truncation of infections. Doubling time is related to growth rate by $\ln(2)/r_t$.